Journal of Structural Geology, Vol. 10, No. 4, pp. 405 to 411, 1988
Printed in Great Britain

0191-8141/88 $03.00 + 0.00

The geometry of planar domino-style normal faults above a dipping basal detachment

GARY J. AXEN*

Department of Geology, Northern Arizona University, Flagstaff, AZ 86011, U.S.A.

(*Received* 6 *January* 1987; *accepted in revised form* 15 *December* 1987)

Abstract—Geometrical analysis of planar domino-style normal faults rooted into a dipping basal detachment fault allows derivation of equations which relate: (1) horizontal extension within the upper plate; (2) dip of the detachment; (3) final fault dips; (4) rotation that faults and beds undergo; and (5) net slip on domino-style faults. Past geometrical models have focused on extremely idealized and non-unique geometries, in which domino-style faults are parallel and similar cut-off points are all at the same elevation after faulting. This corresponds to evenly spaced domino-style faults above a horizontal detachment. Considering non-parallel faults and dipping detachments introduces unique geometries, which allows calculation, for example, of permissible depth ranges to the detachment. Horizontal extension varies significantly: (1) with dip of the detachment; and (2) for synthetic and antithetic cases, in which the domino-style faults dip in the same or opposite direction, respectively, as the detachment. When other factors (e.g. rotation and fault dips) are held constant, horizontal extension greatly increases for moderate detachment dips and moderately decreases for antithetic detachment dips, as compared to the horizontal detachment case. This is important because the synthetic case has been widely reported.

INTRODUCTION

ARRAYS of domino-style normal faults (Fig. 1), which evolve through simultaneous rotation of both faults and beds, have been recognized for over 75 years (Emmons & Garrey 1910). They have been recognized at many scales, with geometries ranging from planar to curviplanar and parallel to non-parallel (e.g. Thompson 1960, Morton & Black 1975, Proffett 1977, Rehrig & Reynolds 1980, Stewart 1980, Chamberlin 1978, 1983, Wernicke & Burchfiel 1982, Gans & Miller 1983, Jackson & MacKenzie 1983, Wernicke *et al.* 1984, 1985, Axen 1986). In the western United States, domino-style normal faults occur above gently dipping detachments (e.g. Wernicke & Burchfiel 1982, Gans & Miller 1983, Wernicke *et al.* 1984, 1985).

Relatively few geometrical analyses have addressed domino-style fault arrays. These fall into two categories: (1) palinspastic analyses (e.g. Proffett 1977, Chamberlin 1983, Gans & Miller 1983, Wernicke *et al.* 1984, 1985, Axen 1986); and (2) simplified geometrical models (e.g. Emmons & Garrey 1910, Thompson 1960, Morton & Black 1975, Wernicke & Burchfiel 1982, Jackson & MacKenzie 1983). In these geometrical models, the domino-style faults are shown as planar, parallel and evenly spaced. All similar cut-off points are shown in cross-section to lie on a horizontal line (Figs. 1 and 2). These near-perfect conditions are seldom substantiated by field investigations. If a detachment underlies the domino-fault array, the conditions above correspond to the detachment being horizontal (Fig. 2). Equations derived from the models give horizontal extension in terms of the fault dip and the amount of rotation that the faults and beds undergo (Fig. 1).

A model is presented here that allows for non-parallel, unevenly spaced domino-style faults and a dipping basal detachment. As well as being somewhat more realistic, the model presented has the advantage of producing unique geometries which allow for rearrangement of the basic equations to solve for quantities previously treated as independent variables, but which may not be known.

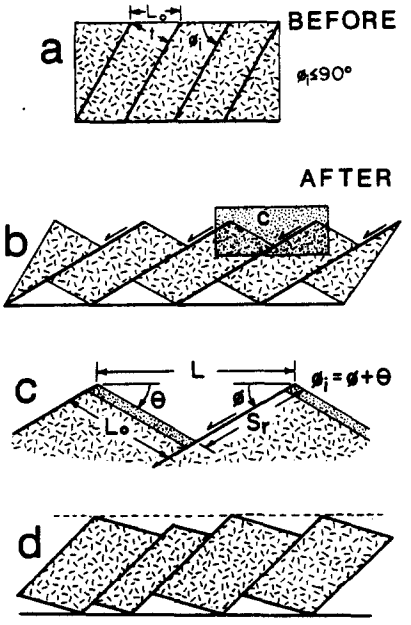

Fig. 1. Parallel domino-style normal faults above a horizontal detachment. (a) Before extension. ϕ_i, initial fault dip; L_0, initial horizontal distance between faults; t, thickness of fault blocks measured perpendicular to faults. (b) After extension. (c) Enlargement of upper portions of two fault blocks, showing variables used in Thompson's (1960) equation for horizontal extension (% H.E.). In this situation % H.E. $= [(L - L_0)/L_0] \times 100 = [\sin(\phi + \theta)/\sin\phi - 1] \times 100$. θ, amount of rotation of beds and faults; ϕ, final fault dip; L, final horizontal distance between faults; S_r, slip due solely to this type of rotational faulting event. (d) Unevenly spaced, parallel, domino-style faults above a horizontal detachment.

*Present address: Department of Earth and Planetary Sciences, Harvard University, Cambridge, MA 02138, U.S.A.

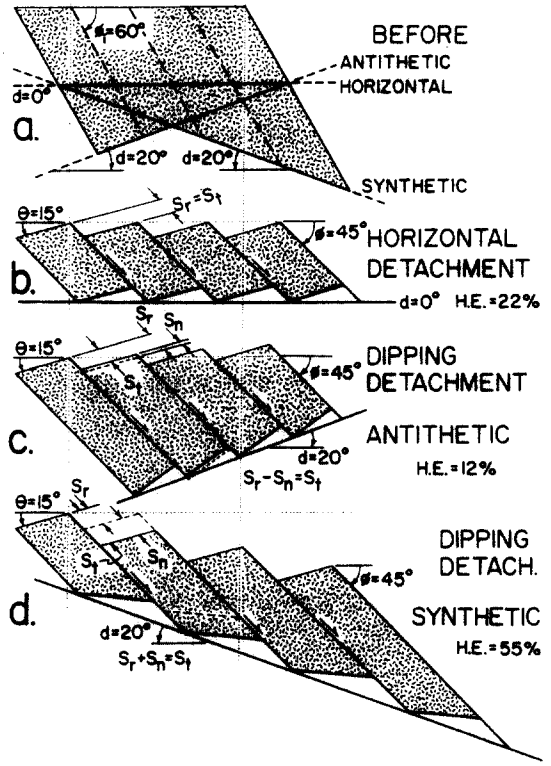

Fig. 2.(a) Three possible initial geometries for domino-style normal fault–detachment systems. The horizontal detachment case (b), the antithetic case (c), and the synthetic case (d) after extension. In (c) and (d) a non-rotational amount of slip, S_n, must be subtracted from or added to the rotational amount of slip, S_r, obtained from (b), to give the total slip, S_t. d, dip of the detachment. The vertical dotted lines show the initial horizontal width of three fault blocks. Note that for identical rotations and fault dips ($\theta = 15°$ and $\phi = 45°$, in this example), widely different amounts of horizontal extension occur.

For example, if domino-style faulting affects previously deformed rocks, bedding dips will not indicate rotations during the domino-style faulting event.

The applicability of these geometrical models is limited to situations where the underlying assumptions are valid. Some of the equations below reasonably approximate naturally occurring geometries. Others are based on assumptions which are rarely or never substantiated by field investigations. The equations presented below represent idealized end-member geometries. Each equation should be evaluated critically with regard to its advantages and limitations in any particular situation. For example, some of the equations may serve well as a guide to cross-section construction, but should be accompanied by section balancing techniques and palinspastic reconstructions. In general, these equations are most applicable to detailed geologic map data, which best allow critical evaluation of the validity of underlying assumptions for a particular case.

ASSUMPTIONS

The geometric models and resulting equations rely on all or some of the assumptions considered below. These assumptions are then evaluated in more detail after the equations have been derived.

Assumption 1. The domino-style normal faults and basal detachment are planar. Gently curviplanar domino-style normal faults have been documented by Proffett (1977), Chamberlin (1978, 1983) and Gans & Miller (1983). These fault planes generally have 5–10° of curvature, which is enough to affect the results of the equations presented. Other workers have documented planar domino-style normal faults, and have produced successful palinspastic reconstructions (Wernicke *et al.* 1984, 1985, Axen 1986) that are consistent with the seismic and geomorphological constraints (Jackson & MacKenzie 1983). Detachments are generally gently curviplanar on a broad scale (e.g. Crittenden *et al.* 1980), but can probably be approximated by a planar surface on the scale of a few hangingwall domino-style normal faults.

Assumption 2. Fault blocks are rigid and do not deform internally. This requirement is most likely to be met at the scale of detailed mapping, but probably is not true at smaller scales. It is most likely to be true at considerable distances above the basal detachment, and is certainly invalid adjacent to the detachment.

Assumption 3. No large translations have occurred on the detachment subsequent to domino-style faulting. The models are based on initial conditions prior to domino-style faulting, and final conditions after domino-style faulting has ceased. Problems occur, for example, if large translations after domino-style faulting leave behind fault-bounded slivers cuts from the base of the domino array (e.g. Lister *et al.* 1984), causing misleading relations between the faults and detachment. However, if the domino-fault array is carried passively after domino-style faulting is over, it can still contain important information about quantities such as detachment dip or depth to the detachment. Alternatively, if large translations are apparent, then the equations will provide constraints on the conditions at the initiation of detachment faulting.

Assumption 4. All of the domino-style faults moved simultaneously. The overprinting of one set of domino-style normal faults by another has been documented in the Yerington District (Proffett 1977), and Snake, Schell Creek and Egan Ranges of Nevada (Gans & Miller 1983). Care must be taken to avoid applying the equations to faults of different generations.

PARALLEL FAULTS

In this section, I consider parallel faults above a dipping detachment, and derive equations for extension, dip of the detachment, and rotation, based on data that can be collected in the field or measured from cross-sections. If domino-style faults are evenly spaced above a horizontal detachment, similar cut-off points of an originally horizontal layer will also form a horizontal datum (Fig. 1). If the domino-style faults are unevenly spaced, however, this is not true.

Dip of the detachment

Figure 2 shows that the total slip, S_t, on domino-style faults above a dipping basal detachment can be thought of in terms of two components: (1) a rotational component, S_r, equal to the slip above a horizontal detachment (Fig. 2b); and (2) a non-rotational component, S_n, due to the different space problem that occurs above a dipping detachment. In the case of synthetic dominoes (Fig. 2d), $S_t > S_r$, and in the case of antithetic dominoes (Fig. 2c), $S_t < S_r$. Likewise, for the synthetic case horizontal extension will be greater than predicted by Thompson's equation (Fig. 1), and less for the antithetic case. For evenly spaced faults, a line drawn through similar, originally horizontal cut-off points will dip in the same direction as the detachment, although by a different amount, allowing the dip direction of the detachment to be determined. However, if the faults are unevenly spaced (Fig. 1d), a line drawn through similar cut-off points will not necessarily dip in the same direction as the detachment. In that case, S_t (measured from sections drawn through the fault in question) must be compared with S_r to determine the dip direction of the detachment. S_r is easily determined by applying the law of sines to the triangle with sides L, L_0, and S_r in Fig. 1(b):

$$S_r = \frac{L_0 \sin \theta}{\sin \phi}. \tag{1}$$

S_r must be calculated using L_0 from the footwall block, because it depends on the thickness of that block (Fig. 1d).

The dip of the detachment, d, can be determined by considering the hypothetical void left at the base of a rigid fault block (Fig. 3). Applying the law of sines to triangle EGI gives

$$S_t = \frac{f_0 \sin \theta}{\sin (\phi - d)}, \tag{2}$$

where $f_0 = \overline{IG}$ is the width of the fault block measured along the detachment surface prior to faulting. From triangle GHI,

$$f_0 = \frac{t}{\sin (\phi_i - d)} = \frac{t}{\sin (\phi + \theta - d)}. \tag{3}$$

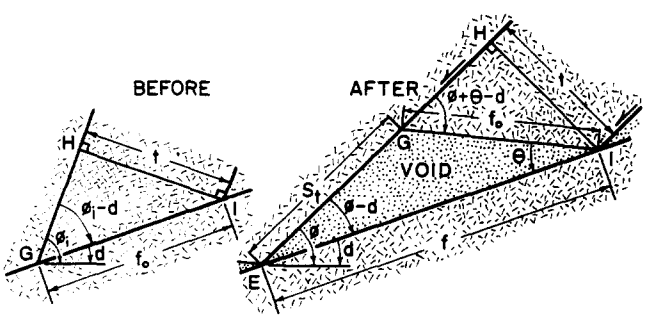

Fig. 3. The hypothetical void space (stippled) left by a domino-style faulting event above a dipping basal detachment. f_0, original, and f, final lengths (respectively) of the block, measured along the detachment; t, thickness of the fault block.

Substituting (3) into (2), rearranging, and solving for d we have

$$d = \phi + \frac{\theta}{2} - \frac{1}{2} \arccos \left[\cos \theta - \frac{2t \sin \theta}{S_t} \right] \tag{4}$$

where d is defined as positive for the synthetic case and negative for the antithetic case.

The depth to the detachment cannot be uniquely determined for parallel faults. This is not true for non-parallel faults, as will be shown below.

Rotation

In areas where rocks were deformed prior to domino-style normal faulting, or in areas of non-stratified rocks, the rotation, θ, must be determined. This can be obtained from the total slip, thickness of the footwall block, and dip of the detachment. Applying the law of sines to triangles in Fig. 3 gives $S_t/\sin \theta = f_0/\sin (\phi - d)$. Also, $f_0 = t/\sin (\phi + \theta - d)$.

Combining these two and simplifying gives

$$\theta = \arctan \left\{ \frac{S_t[1 - \cos (2\phi - 2d)]}{2t - S_t \sin (2\phi - 2d)} \right\}. \tag{5}$$

Amount of extension

Per cent horizontal extension (% H.E.) can be written as a function of ϕ and θ. From Fig. 4 it is seen that

$$L'' = L' \pm \Delta L \tag{6}$$

and that

$$\Delta L = S_n \cos \phi. \tag{7a}$$

From the law of sines,

$$L' = \frac{L_0 \sin (180 - \phi - \theta)}{\sin \phi} = \frac{L_0 \sin (\phi + \theta)}{\sin \phi}. \tag{7b}$$

The per cent horizontal extension is given by

$$\%\ \text{H.E.} = \left(\frac{L'' - L_0}{L_0} \right) \times 100 = \left(\frac{L''}{L_0} - 1 \right) \times 100. \tag{8}$$

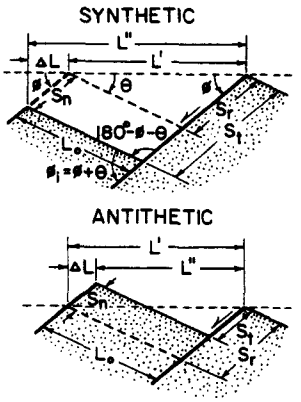

Fig. 4. Synthetic and antithetic cases of parallel, domino-style normal faults above a dipping detachment. L' is the horizontal distance between faults that would result if the detachment were horizontal. L'' is the horizontal distance between faults above a dipping detachment and ΔL is the difference.

Combining equations (6)–(8) gives

$$\% \text{ H.E.} = \left[\frac{\sin(\phi + \theta)}{\sin \phi} + \frac{S_n}{L_0} \cos \phi - 1\right] \times 100. \tag{9}$$

S_n is determined by subtracting S_r, calculated from (1) for the hangingwall block, from S_t, which is measured. S_n is defined as positive for the synthetic case, and negative for the antithetic case.

Although (9) is useful for application to geological maps and sections, it is convenient to consider % H.E. as a function of rotation and fault dips only. For this, we need an expression for S_n in terms of θ, ϕ and d. From Fig. 3 it can be seen that $S_t = \overline{EH} - \overline{GH}$. Also,

$$\overline{EH} = t \cot(\phi - d)$$

and

$$\overline{GH} = t \cot(\phi + \theta - d).$$

Therefore,

$$S_t = \overline{EH} - \overline{GH} = t[\cot(\phi - d) - \cot(\phi + \theta - d)]. \tag{10}$$

S_r is obtained from (1) for the hangingwall block, and $S_n = S_t - S_r$, so

$$S_n = t[\cot(\phi - d) - \cot(\phi + \theta - d)] - \frac{L_0 \sin \theta}{\sin \phi}. \tag{11}$$

Substituting (11) into (9) and simplifying gives

$$\% \text{ H.E.} = \left\{\cos \theta + \frac{t \cos \theta}{L_0}[\cot(\phi - d) - \cot(\phi + \theta - d)] - 1\right\} \times 100. \tag{12}$$

For evenly spaced parallel faults, $t/L_0 = \sin \phi_i = \sin(\phi + \theta)$ (Fig. 1), so (12) simplifies to

$$\% \text{ H.E.} = \{\cos \theta + \sin(\phi + \theta) \cos \phi [\cot(\phi - d) - \cot(\phi + \theta - d)] - 1\} \times 100. \tag{13}$$

Figure 5 is a plot of % H.E. calculated using (13), for a variety of detachment dips, d, for the case where $\phi_i = 60°$, and θ varies from 0° to 25°. Note the dramatic increase in extension for the synthetic cases with low to moderate detachment dips and rotations when compared to the horizontal detachment case ($d = 0°$).

Per cent extension parallel to the detachment (% E_d) can also be figured by considering the void space left below the rigid fault block (Fig. 3). Equation (8) is used, with $L'' = \overline{EI}$ and $L_0 = \overline{GI}$. Then,

$$L'' = \overline{EI} = \frac{t}{\sin(\phi - d)}$$

and

$$L_0 = \overline{GI} = \frac{t}{\sin(\phi_i - d)} = \frac{t}{\sin(\phi + \theta - d)}.$$

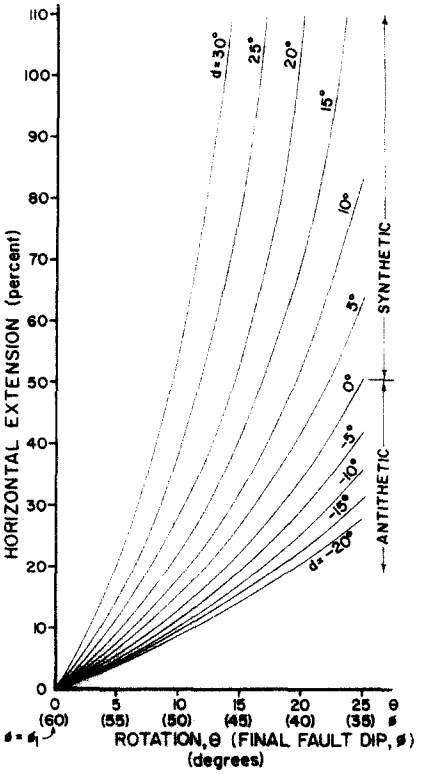

Fig. 5. Example of how horizontal extension varies due to changing dip of the detachment, d, for parallel faults with initial dips of 60°, and various rotations.

Substituting these into (8) gives

$$\% E_d = \left[\frac{\sin(\phi + \theta - d)}{\sin(\phi - d)} - 1\right] \times 100. \tag{14}$$

Extension parallel to the detachment can differ markedly from the horizontal extension. In the antithetic case % E_d can be zero for faults that rotate through a line perpendicular to the detachment. Calculation of % E_d may be useful for determining a minimum offset on a detachment fault, or for economic studies of mineralized detachment zones.

NON-PARALLEL FAULTS

When domino-style normal faults are observed in the field, they are generally not parallel (e.g. Wernicke *et al.* 1984, Axen 1986). The geometry of non-parallel domino-style faults is complicated compared to their parallel counterparts, because the thickness of the blocks changes with depth. This is dealt with below, and is somewhat offset by the advantage of allowing a unique solution for depth to the basal detachment.

Dip of the detachment

The easiest method for determining the dip of the detachment requires use of three adjacent domino-style

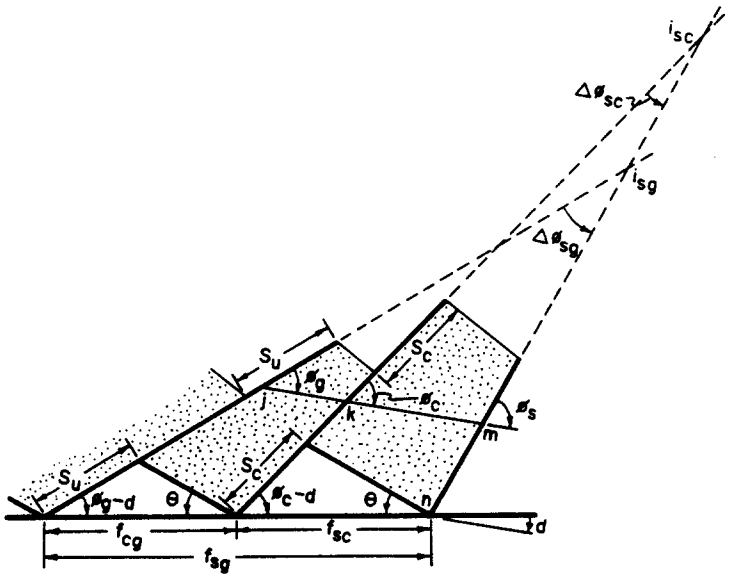

Fig. 6. Non-parallel domino-style faults above a dipping detachment. S_u, S_c, slip on the upper and central faults, respectively; ϕ_g, ϕ_c, ϕ_s, dip of the gentler, central and steeper faults, respectively; i_{sc}, i_{sg}, intersection points of the projections of the steeper and central faults, and steeper and gentler faults, respectively. $\overline{jm}$ is an arbitrary horizontal line drawn through the cross-section.

faults and the two included fault blocks (Fig. 6). The following can be obtained from the law of sines:

$$\overline{mi}_{sc} = \overline{km} \sin(\phi_c)/\sin(\Delta\phi_{sc}),$$
$$\overline{mi}_{sg} = \overline{jm} \sin(\phi_g)/\sin(\Delta\phi_{sg}),$$
$$\overline{ni}_{sc} = f_{sc} \sin(\phi_c - d)/\sin(\Delta\phi_{sc}),$$
$$\overline{ni}_{sg} = f_{sg} \sin(\phi_g - d)/\sin(\Delta\phi_{sg}),$$
$$f_{cg} = S_u \sin(\phi_g + \theta - d)/\sin\theta$$
$$f_{sc} = S_c \sin(\phi_c + \theta - d)/\sin\theta.$$

Because $\overline{i_{sg}i_{sc}} = \overline{mi}_{sc} - \overline{mi}_{sg} = \overline{ni}_{sc} - \overline{ni}_{sg}$ and $f_{sg} = f_{cg} + f_{sc}$, the above equations can be combined and simplified to give

$$\frac{\overline{km}\sin\phi_c}{\sin(\Delta\phi_{sc})} - \frac{\overline{jm}\sin\phi_g}{\sin(\Delta\phi_{sg})} = \frac{S_c \sin(\phi_c + \theta - d)\sin(\phi_c - d)}{\sin\theta \sin(\Delta\phi_{sc})} - \frac{\sin(\phi_g - d)[S_c \sin(\phi_c + \theta - d) + S_u \sin(\phi_g + \theta - d)]}{\sin\theta \sin(\Delta\phi_{sg})}. \quad (15)$$

An analogous solution for the case where the upper fault is the steeper fault gives

$$\frac{\overline{km}\sin\phi_c}{\sin(\Delta\phi_{sc})} - \frac{\overline{jm}\sin\phi_g}{\sin(\Delta\phi_{sg})} = \frac{S_u \sin(\phi_s + \theta - d)\sin(\phi_c - d)}{\sin\theta \sin(\Delta\phi_{sc})} - \frac{\sin(\phi_g - d)[S_u \sin(\phi_s + \theta - d) + S_c \sin(\phi_c + \theta - d)]}{\sin\theta \sin(\Delta\phi_{sg})}. \quad (16)$$

Although these equations are too cumbersome for quick use, d can be found by iteration. Two solutions can occur, one synthetic and one antithetic, but one can be discarded on geometric grounds (for example, $\overline{jm}$ will end up going through or below the detachment, or the wrong solution will give too steep a dip for the detachment). The central fault can have any dip, as long as it is not parallel to either of the other faults and can be inferred to intersect the detachment (for the latter reason, downward-widening fault blocks are better to use).

Depth to the detachment

Because fault-block thickness varies for non-parallel faults, the size of the hypothetical void at the base of a tapering block is uniquely determined by the thickness of the block at its base. The basal thickness is measured from the intersection of the lower bounding fault with the detachment, along a line perpendicular to the upper bounding fault (see the right block in Fig. 6). It can be determined algebraically if S_t, d, θ and ϕ_u (the dip of the upper bounding fault) are known. Once the basal thickness is obtained, the dimensions of the block are fully known, so that maximum and minimum depths to the detachment can be found. The maximum depth corresponds to the bases of the rigid fault blocks, and the minimum depth corresponds to the tops of the hypothetical void triangles. Equation (4) can be used to this end, by rearranging to solve for t:

$$t = \frac{S_t \sin(\phi_u + \theta - d)\sin(\phi_u - d)}{\sin\theta}. \quad (17)$$

Estimating the amount of extension

Horizontal extension for non-parallel faults can be estimated using equation (9), but one must be sure to use ϕ from the fault below the block in question in equation

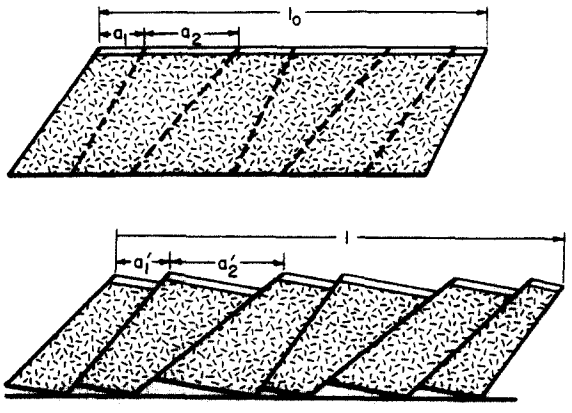

Fig. 7. Non-parallel domino-style faults above a horizontal detachment. See text for explanation.

(1) for S_r. Similarly, equation (12) can be used, but the thickness (t) used must be that obtained from equation (17) for the footwall block. Extension parallel to the basal detachment can be estimated using equation (14) directly.

The amount of extension is strongly dependent on the basal thickness of the block below the fault in question. For downward-widening blocks, S_n and S_t will be large, and for downward-narrowing blocks they will be small. In the extreme latter case the faults will intersect at the detachment, and slip will be zero, unless significant distortion of the block occurs as it moves through the bend between the domino-style fault and the detachment.

Unlike parallel domino-style faults, where % H.E. is the same for all blocks regardless of dimensions, non-parallel faults each cause a different % H.E. between cut-off points. Therefore, to arrive at the % H.E. across an array of non-parallel domino-style faults, one must do a weighted summation of extension due to each fault in the array.

Figure 7 shows a set of domino-style faults with non-parallel dips above a horizontal detachment. Thompson's (1960) equation (Fig. 1) is used to obtain the horizontal extension of individual fault blocks, and each individual extension is multiplied by the fraction of the final total length to which it contributed. The total extension across the length, l, of the extended section (Fig. 7) is:

$$\% \text{ extension} = \sum_{m=1}^{n} \left[\frac{\sin(\phi_m + \theta)}{\sin \phi_m} - 1 \right] (e_m) \times 100.$$

where ϕ_m is the final dip of the mth fault and e_m is the fraction of the total length of the extended section which is due to each fault:

$$e_1 = \frac{a_1'}{l} \quad \text{and} \quad \frac{a_2'}{l},$$

where a_1' and a_2' are horizontal distances between similar piercing points. Similar summations can be done for non-parallel faults above dipping detachments using equations (9) or (12).

DISCUSSION

The equations presented above are most useful for structural analysis of detailed maps. In particular they can be used to provide some subsurface information when other considerations suggest that a detachment exists at depth. The equations giving dip of, and depth to, a detachment might be particularly useful in minerals exploration for ores deposited adjacent to detachment faults. By analyzing several domino-style faults, one could potentially characterize irregularities in the dip of the detachment, such as have been imaged seismically (e.g. Allmendinger *et al.* 1983).

Uplift and warping of detachment faults due to isostatic rebound following tectonic denudation (e.g. Spencer 1982, 1984) should be considered when applying these equations. A broadly warped detachment can probably be approximated as planar over a sufficiently small area. If uplift (or other subsequent deformation) passively rotates the part of the domino-style fault–detachment system being considered, then the geometries described here still hold, because fault-to-detachment angles will not be changed. This has the effect of automatically including changes in the per cent horizontal extension which are due to the passive rotation. Equations for depth to, or dip of, the detachment will simply yield post-passive-rotation figures.

These equations could also be useful in drawing sections across unexposed domino-style faults. If adjacent faults are well enough exposed to determine the dip of the underlying detachment, then equations (4), (15) and (16) can be used to determine the dip of the unexposed fault.

As with any theoretical model, these equations are only as good as the underlying assumptions. Care should be taken to ensure that only planar faults are used. This may be true if rotations (bedding dips) across faults are constant: differential rotations require curviplanar or splayed faults. The converse is not necessarily true, as only small amounts of internal distortion of blocks rotated by gently curviplanar faults can result in essentially parallel bedding dips across faults (e.g. Proffett 1977, Gans & Miller 1983). Palinspastic reconstruction can help to determine if faults are planar or curved (e.g. Axen 1986). In general, this type of theoretical analysis should be accompanied by palinspastic reconstruction of balanced cross-sections. When the three techniques are played against one another, they provide a powerful tool.

Clearly a major assumption that cannot be true in any but the shallowest natural settings is that rigid blocks require a void to open at depth (Fig. 3). Field observations indicate that, at best, the upper parts of domino blocks behave rigidly. The 'void problem' is apparently commonly 'solved' by formation of thick breccia zones (e.g. Axen 1986, Axen & Wernicke 1986), downward-splaying faults (e.g. Gans & Miller 1983) or formation of chaos structure (e.g. Noble 1941, Wernicke & Burchfiel 1982). Although slip measured at the surface should

equal total slip near the detachment, the hypothetical voids are probably reduced in size and 'filled' by rock transferred from areas that would form the lower corners of the blocks. The possible range of depth to the detachment, based upon calculation of the basal thickness of fault blocks, can probably be constrained to the range from the tops to the bottoms of the voids. Because brecciation causes volume increase, deeper estimates within this range may be closer. Simple area balancing of the voids and protruding lower corners of the blocks should be attempted.

The space problem at the base of fault blocks becomes greater with increasing rotation. When compared to the problem for faults above a horizontal detachment, this effect is somewhat lessened for faults antithetic to the basal detachment, and is greatly increased for the synthetic case (Fig. 2). Large rotations on domino-style faults probably require: (1) intense internal deformation of blocks; (2) curviplanar or splaying faults, which may result from (1), and/or (3) that fault blocks thin downward to a small basal thickness. Therefore these equations are best applied to faults which have undergone no more than moderate rotations. Such internal deformation would not necessarily be present far from the detachment, and might not be noticeable at the surface. This introduces additional uncertainty into calculations of depth to the detachment.

For downward-thickening fault blocks the basal space problem is larger and for downward-thinning blocks it is smaller. For best results in calculations of d or depth to the detachment, several differently shaped blocks should be used if possible. This approach will also help to avoid spurious results from faults which intersect above the detachment.

Because many of the equations are based on triangles with acute angles, small errors in measurement of the various angles, the total slip, or the thickness of blocks can introduce fairly large errors. It is advisable to do the calculations for (1) the best measurements and (2) the acceptable range of measurements, substituted so as to maximize and minimize the quantity being calculated. For small errors in a single measurement, the error introduced into the result of the equations presented tends to be of the same order. However, for compounding errors of 1–2° in angles and less than 10% in slip measurements, the errors propagated can be problematically large.

The effect of the dip of the basal detachment on estimates of horizontal extension deserves emphasis. For given rotations and fault dips, the extension will be significantly larger in the synthetic case, or moderately smaller in the antithetic case, when compared to the extension above a horizontal detachment (Figs. 2 and 5). This is important because the synthetic case is commonly reported.

Acknowledgements—The manuscript has greatly benefited from the careful reviews of J. Bartley, G. A. Davis, P. Delaney, J. Fryxell and P. Gans. Field work in the Ely Springs Range area, Nevada, which led to the models presented here, was supported by the Organized Research Committee of Northern Arizona University.

REFERENCES

Allmendinger, R. W., Sharp, J. W., Von Tish, D., Serpa, L., Brown, L., Kaufman, S., Oliver, J. & Smith, R. B. 1983. Cenozoic and Mesozoic structure of the eastern Basin and Range province, Utah, from COCORP seismic-reflection data. *Geology* **11**, 532–536.

Axen, G. J. 1986. Superposed normal faults in the Ely Springs Range, Nevada: estimates of extension. *J. Struct. Geol.* **8**, 711–713.

Axen, G. J. & Wernicke, B. P. 1986. Structural characteristics of large-scale upper crustal extension within an older foreland thrust belt. *Geol. Soc. Am. Abs. w. Prog.* **18**, 530.

Chamberlin, R. M. 1978. Structural development of the Lemitar Mountains, an intrarift tilted fault block uplift, central New Mexico. In: *Proceedings of the International Symposium on the Rio Grande Rift, Sante Fe, New Mexico*, Conference proceedings LA-7487-C, Los Alamos Scientific Laboratory, Los Alamos, New Mexico, 22–24.

Chamberlin, R. M. 1983. Cenozoic domino-style crustal extension in the Lemitar Mountains, New Mexico: a summary. In: *Guidebook, 34th Field Conference, Socorro Region II* (edited by Chapin, C. E. & Callender, J. F.). New Mexico geol. Soc., Socorro, New Mexico, 111–118.

Crittenden, M. D., Coney, P. J. & Davis, G. H. 1980 (editors) *Cordilleran Metamorphic Core Complexes. Mem. geol. Soc. Am.* **153**, 490.

Emmons, W. H. & Garrey, G. H. 1910. General Geology. In: *Geology and Ore Deposits of the Bullfrog District* (edited by Ransome, F. L.). *Bull. U.S. geol. Surv.* **407**, 19–89.

Gans, P. B. & Miller, E. L. 1983. Style of mid-Tertiary extension in east-central Nevada. In: *Geological Excursions in the Overthrust Belt and Metamorphic Core Complexes of the Intermountain Region* (edited by Nash, W. P. & Gurgel, K. D.). *Utah geol. & Mineral. Surv. Special Studies* **59**, 108–160.

Jackson, J. & MacKenzie, D. 1983. The geometrical evolution of normal fault systems. *J. Struct. Geol.* **5**, 471–482.

Lister, G. S., Davis, G. A., McClelland, W. C. & Marcott, D. T. 1984. Complexities in the evolution of low-angle crustal shear zones during continental extension. *Geol. Soc. Am. Abs. w. Prog.* **16**, 577.

Morton, W. H. & Black, R. 1975. Crustal attenuation in Afar. In: *Afar Depression of Ethiopia, Inter-Union Commission on Geodynamics* (edited by Pilgar, A. & Rosler, A.). International Symposium on the Afar Region and Related Rift Problems, E. Schweizerbart'sche Verlagsbuchhandlung, Stuttgart, Germany, Proceedings, Scientific Report No 14, 55–65.

Noble, L. F. 1941. Structural features of the Virgin Spring area, Death Valley, California. *Bull. geol. Soc. Am.* **52**, 941–1000.

Proffett, J. M., Jr. 1977. Cenozoic geology of the Yerington district, Nevada, and implications for the nature and origin of Basin and Range faulting. *Bull. geol. Soc. Am.* **88**, 247–266.

Spencer, J. E. 1982. Origin of folds of Tertiary low-angle fault surfaces, southeastern California and western Arizona. In: *Mesozoic–Cenozoic Tectonic Evolution of the Colorado River Region, California, Arizona and Nevada* (edited by Frost, E. G. & Martin, D. L.). Cordilleran Publishers, San Diego, 123–134.

Spencer, J. E. 1984. Role of tectonic denudation in warping and uplift of low-angle normal faults. *Geology* **12**, 95–98.

Stewart, J. H. 1980. Regional tilt patterns of late Cenozoic Basin–Range fault blocks, western United States. *Bull. geol. Soc. Am.* **91**, 460–464.

Thompson, G. A. 1960. Problem of late Cenozoic structure of the Basin Ranges. In: *Proceedings of the 21st International Geological Congress*. Det Berlingski Bogtrykkeri, Copenhagen, **18**, 62–68.

Wernicke, B. P. & Burchfiel, B. C. 1982. Modes of extensional tectonics. *J. Struct. Geol.* **4**, 105–115.

Wernicke, B. P., Guth, P. L. & Axen, G. J. 1984. Tertiary extensional tectonics in the Sevier belt of southern Nevada. In: *Western Geological Excursions, Guidebook for 1984 Geological Society of America Annual Meeting* (edited by Lintz, J., Jr), Vol. 4. Mackay School of Mines, Reno, Nevada, 473–510.

Wernicke, B. P., Walker, J. D. & Beaufait, M. S. 1985. Structural discordance between Neogene detachments and frontal Sevier thrusts, central Mormon Mountains, southern Nevada. *Tectonics* **4**, 213–246.